Measurement of the matched spot size in a capillary discharge waveguide with a collimated laser

Jiaqi Liu,[1,2] Wentao Li,[1,3,a] Jiansheng Liu,[1,4,b] Zhiyong Qin,[1,2] Wentao Wang,[1] Rong Qi,[1] Zhijun Zhang,[1] Changhai Yu,[1] Ming Fang,[1,2] Ke Feng,[1,2] Ying Wu,[1,2] Cheng Wang,[1] and Ruxin Li[1,4,5,c]

[1]*State Key Laboratory of High Field Laser Physics, Shanghai Institute of Optics and Fine Mechanics, Chinese Academy of Sciences, Shanghai 201800, China*
[2]*University of Chinese Academy of Sciences, Beijing 100049, China*
[3]*Department of Physics, SUPA and University of Strathclyde, Glasgow G4 0NG, United Kingdom*
[4]*IFSA Collaborative Innovation Center, Shanghai Jiao Tong University, Shanghai 200240, China*
[5]*School of Physical Science and Technology, ShanghaiTech University, Shanghai 200031, China*

(Received 18 January 2018; accepted 23 July 2018; published online 3 October 2018)

Measurement of the matched spot size in the hydrogen-filled capillary discharge waveguide based on the spot size oscillation of a collimated laser is presented in this paper. The spot size oscillation trace is retrieved from the laser modes measured at the exits of discharged capillaries of different lengths under the same discharge conditions. With the gas pressure, peak discharge electric current and capillary radius fixed, the radial density profiles are identical in all the discharged capillaries. The measured laser modes are equivalent to the evolution at discrete positions in a long plasma channel. Compared to former researches based on the spot size at the capillary exit, this method is not affected by the multiple solution problem. The use of a collimated laser eliminates the influences of the divergence angle on the fitting accuracy. By this means, the matched spot sizes of hydrogen-filled capillary discharge waveguides under different gas pressures (5-20mbar) are measured. The results can provide a spot size reference for the laser wakefield accelerator guided in a plasma channel. https://doi.org/10.1063/1.5022817

I. INTRODUCTION

Laser wakefield accelerators (LWFAs) have received considerable attention as potential high-quality next-generation electron beam sources.[1–4] Because of its high acceleration gradient, energetic electron beams can be generated in a compact distance. To obtain multi-GeV-scale energy, long distance acceleration remains to be a challenge owing to laser diffraction and short dephasing length. The self-guided LWFA was proposed as an improved scheme, and has generated an electron beams beyond 1 GeV.[5] However, the self-guiding over the entire plasma region only lasted for ≃ 15 vacuum Rayleigh lengths because of the laser depletion in high-density plasma. To achieve a better guiding behavior, the capillary discharge waveguide has been considered feasible.[6–9] In the gas-filled capillary discharge, the plasma channel is formed by the temperature profile during discharge, which is higher in the center due to the Ohmic heating effect of plasma and drops radially because the heating is

[a]wentao.li@strath.ac.uk
[b]michaeljs_liu@siom.ac.cn
[c]ruxinli@mail.siom.ac.cn

balanced by heat conduction to the capillary wall.[10,11] As the gas pressure is almost uniform, the radial plasma density has quasi-quadratic profile.

A Gaussion intensity laser pulse distributed as $I = I_0 \exp\left(-2r^2/r_i^2\right)$ can be well guided in a plasma channel with a parabolic density distribution as $n(r) = n_0 + (r/r_m)^2 n_d$ $(r \le r_m)$ if the waist radius r_i equals the matched spot size $r_m = (\pi r_e n_d)^{-1/2}$,[11–15] where n_0 is the on-axis density, n_d is the density depth (density difference between the axis and r_m), and r_e is the classical electron radius. To achieve a better guiding behavior, optical schemes have been proposed to diagnose the capillary discharge waveguide. Longitudinal interferometry offers an intuitive pattern of the density profile, which is only accurate for capillaries of millimeter-scale length and the result is affected by the end effect.[16] Transverse interferometry provides the transverse density profile, whereas it requires square capillaries.[17] The laser centroid oscillation measurement can be used to determine the matched spot size and channel profile, however the experimental result is affected by the incident angle.[18,19] r_m can also be determined from the spot size oscillation in the plasma channel, such as measuring laser spot size at the capillary exit.[20] But it is sensitive to the focal position shift of the laser. Moreover, more than one solution to the matched spot size might exist for a specific exit spot size, which also introduces measurement inaccuracy. On the other hand, continuous measurement of the laser spot sizes along the discharged capillary is difficult.

In this paper, a method based on the spot size oscillation is presented to diagnose the matched spot size r_m of the hydrogen-filled capillary discharge waveguide, which is aimed to offer a spot size reference for the channel-guided LWFAs and obtain high-energy electron beams. The spot sizes are measured at the exit of capillaries of different lengths under the same discharge conditions, including the diameter of hole (500 μm), discharge current profile (80 A peak current), and filling gas pressure (5 – 20 mbar). This method relies on the fact that the radial density profiles in hydrogen-filled capillary discharge waveguides mainly depend on the three parameters in absence of the longitudinal flow.[11] The measured spot sizes are identical to those at discrete positions of a long waveguide under the same discharge conditions. Then the spot size oscillation trace is obtained by fitting the experimental data to the theoretical oscillation formula. Adoption of a collimated laser eliminates the influence of the divergence angle of the probe laser to ensure the fitting accuracy. Moreover, this method avoids multi-solution inaccuracy. The probe laser is low in intensity ($7 \times 10^{10}\ W/cm^2$), which avoids the influence of the relativistic effects. The diagnostic shows that r_m and n_d were 41.8 μm under a pressure of ~20 mbar ($9.7 \times 10^{17}\ cm^{-3}$). Further, this method was used to measure the matched spot sizes of the discharged waveguides in lower plasma density. The results were 46.0 μm at ~15 mbar ($7.0 \times 10^{17}\ cm^{-3}$), and 48.64 μm at ~5 mbar ($2.4 \times 10^{17}\ cm^{-3}$).

II. COLLIMATED LASER PROPAGATION IN A PLASMA CHANNEL

The low-intensity collimated probe laser in experiment is aimed at minimizing the influence of the divergence angle r_i' of a focal laser, which is caused by the position inaccuracy Δz between the focal position and the entrance of the plasma channel as $r_i' \approx \lambda^2 \Delta z / \pi^2 r_{i0}^3$. Considering a Gaussian intensity profile laser with a beam waist radius of r_{i0} and divergence angle of r_i' at the channel entrance, according to Ref. 23, the spot size r_o after a propagation distance d is formulated as

$$r_o^2 \approx \frac{1}{2}\left(r_{i0}^2 + \frac{\pi^2 r_{i0}^4 r_i'^2}{\lambda^2} + \frac{r_m^4}{r_{i0}^2}\right) + \frac{1}{2}\left(r_{i0}^2 + \frac{\pi^2 r_{i0}^4 r_i'^2}{\lambda^2} - \frac{r_m^4}{r_{i0}^2}\right)\cos(kd) + \frac{\pi r_{i0} r_m^2 r_i'}{\lambda}\sin(kd), \qquad (1)$$

where λ is the wavelength of the probe light and $k = 2\lambda/\pi r_m^2$. The spot size oscillates periodically inside the plasma channel. Although the oscillation duration is independent of r_i', the oscillation amplitude will be enlarged if r_i' at the plasma channel entrance is not zero. As shown in Fig. 1 with $\lambda = 0.8\ \mu m$, $r_{i0} = 25\ \mu m$ and $r_m = 45\ \mu m$, the spot size oscillation amplitude for $r_i' = 8\ mrad$ is 6.45 μm larger than that for $r_i' = 0$. The amplitude enlargement will introduce error in determination of r_m, because r_m is related to the extreme values of the spot size oscillation trace. To minimize the influence of the divergence angle, a collimated laser is considered as a promotive scheme because

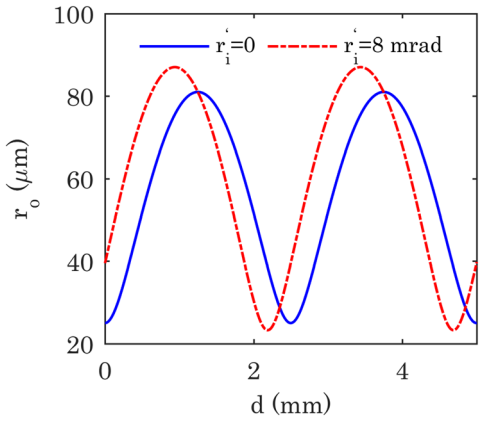

FIG. 1. Spot size oscillation trace from Eq. (1) for different r_i' with $\lambda = 0.8\,\mu m$, $r_{i0} = 25\,\mu m$ and $r_m = 45\,\mu m$.

$r_i' \approx 0$. Therefore, Eq. (1) can be simplified to a common form as in Ref. 19:

$$r_o^2 = \frac{1}{2}\left(r_{i0}^2 + \frac{r_m^4}{r_{i0}^2}\right) + \frac{1}{2}\left(r_{i0}^2 - \frac{r_m^4}{r_{i0}^2}\right)\cos(kd). \tag{2}$$

Equation (2) indicates that the spot size oscillation inside the plasma channel is independent of r_i' for a collimated laser. Additionally, the oscillation described by Eq. (2) is unique for a specific r_m. Therefore, the multi-solution problem can be avoided. In this paper, the spot size oscillation trace is retrieved by fitting Eq. (2) to the spot sizes of the laser modes measured at the exits of the capillaries.

III. EXPERIMENTAL SETUP

The experiment was performed with a 10 Hz pulsed Nd:YAG laser at 532 nm as shown in Fig. 2. The divergence of the incident laser was less than 50 μrad, and it can be considered collimated taking into account the 500 μm diameter hole and centimeter-scale length of the capillary. The pulse had an energy of 150 mJ, full width at half-maximum duration of 10 ps, and beam waist radius of 2.5 mm

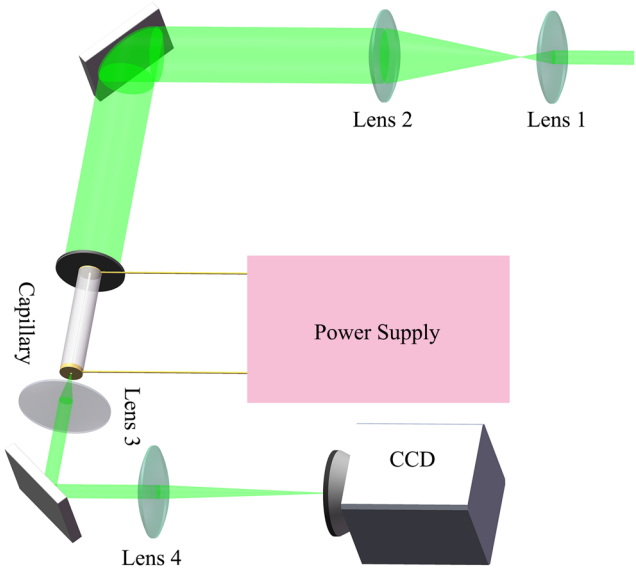

FIG. 2. Experimental setup for the matched spot size measurement.

at $1/e^2$ of the peak intensity, corresponding to an intensity of $7 \times 10^{10}\ W/cm^2$, which is lower than the ionization threshold of hydrogen of $1 \times 10^{14}\ W/cm^2$. The capillary was made of fused silica. The hydrogen gas was filled in from two slots located 1 mm from each of the capillary ends. The gas pressure was roughly detected by attaching a micro gas pressure sensor to one of the capillary ends, which varied in a range between 5 and 20 mbar. The on-axis plasma densities were measured by the Stark broadening of the H-alpha spectrum line at the exit of the capillary.[21,22] The peak discharge current was fixed at 80 A for all capillaries by tuning the voltage. The laser modes at exits of capillaries were recorded by a CCD camera after being magnified 6 times. The laser spot size were determined by fitting the laser intensity to a Gaussian form.

Before the measurement, the capillary was aligned by observing the laser modes at the exit of the capillary. This process is necessary because good alignment will reduce the errors caused by incident angle. Although the incident angle does not affect the spot size oscillation directly, it will introduce errors in the spot size measurement when fitting the intensity profile of the laser modes to a Gaussian form. The capillary is first roughly aligned by observing the transmitted laser energy and the laser mode at the exit of the capillary while adjusting its position and angle. A further alignment is achieved if the transmitted laser energy's evolution is the same for a same radial position shift in any direction. Since the laser energy stability is with 1%, the transmitted energy variates obviously when the shifting distance is as large as the beam waist radius. The best alignment is achieved when the transmitted laser energy and the output laser mode changes in the same way with rotation of the angle or a shift in the position by the same degree in any radial direction.

IV. RESULT AND DISCUSSION

The radial density profile was kept identical for capillaries of different lengths by maintaining the same peak discharge current and gas pressure. This is because radial density variation depends on the radial temperature profile and on-axis density.[11] And the radial temperature profile depends on the discharge current and capillary radius. In experiments, the capillary discharge was performed with a peak electric current of 80 A by tuning the voltage. The discharge current profiles in capillaries of 2 cm to 8 cm under a 20-mbar pressure are shown in Fig. 3(a). For all capillaries, the discharge current profile were similar in shape before 1000 *ns*, which began to rise at 90 *ns* and reached the current peaks at ~490 *ns*. The on-axis electron density distributions at 20 mbar along capillaries of 3 cm and 6cm lengths at 500 *ns* were measured by Stark line broadening, which are plotted in Fig. 3(b). The axial density profile was almost uniform from 2 mm to 28 (58) mm away from the entrance of a 3 (6) cm capillary. The average electron density was $9.7 \times 10^{17}\ cm^{-3}$, which is close to the theoretical electron density assuming full ionization. The error bars were the deviation ranges of the data measured at each position. It is worth noting that the electron density has a falling ramp near the gas slots, which is also known as end effect.[24] However, the length of the density ramp is ~2 *mm*, which has limited effects on the spot sizes as will be discussed. Since the discharge current profiles and on-axis density are similar for capillaries of different lengths under the same discharge conditions, the radial density distribution can be considered to be the same. And the laser modes at

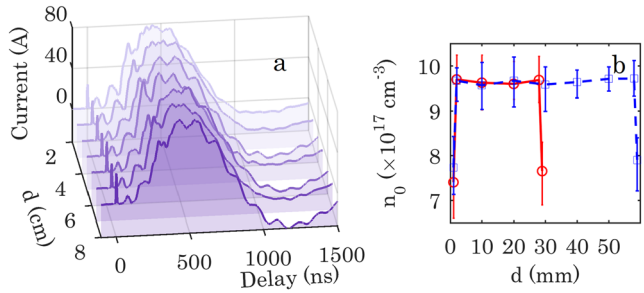

FIG. 3. (a) Discharge electric current profiles in capillaries of different lengths. (b) On-axis electron density along the capillaries of 3 cm (red) and 6 cm (blue) lengths.

the exit of capillaries of different lengths are identical to the laser evolution at discrete positions in a long channel.

The plasma channel only exists around the electric current peak, which could be recognized from the measured laser modes. The laser modes from 100 to 1000 *ns* at the exit of a 2 *cm* capillary under a 20-mbar pressure are plotted in Fig. 4. The radial intensity profile (red trace) was obtained by summing the central 30 rows of pixels of the images recorded by CCD. At the beginning (100 *ns*) and end (1000 *ns*) of the discharge when the current was low and the ionized electrons were rare, the laser intensity profile was almost flat in the central range within a 140 μm radius. When the current and electron density continued to rise (200 *ns* and 900 *ns*), the light was separated into a circumjacent ring and a central circle with similar intensities. And the size of the circular region kept changing during the discharge. This might be because the radial density profile has not formed a channel shape yet when the hydrogen was not fully ionized. If the discharge current rose closer to the peak (300 *ns* and 800 *ns*), the central circle was further focused to an almost unchanged value while the intensity of the circumjacent light became much lower, which indicated the existence of a plasma channel. In this time range, the spot sizes of the laser modes were obtained by fitting the intensity profile of the central light to a Gaussian form, as the dashed yellow traces in Figs. 4(c) and (d). The spot size oscillation trace inside a long discharged capillary was retrieved by fitting Eq. (2) to the measured laser spot sizes at the same delay for different capillaries.

r_{i0} and r_m are determined by fitting all the laser sizes measured at the same time to Eq. (2) using the non-linear least square algorithm. For instance, the spot sizes measured at 500 *ns* for capillary lengths from 3 to 8 *cm* at a 0.5 cm interval are plotted in Fig. 5(a). The error bars represent the deviation range of the measured spot sizes from the average value at each interval. Fitting all the measured data to Eq. (2) with the same weight, the spot size oscillation trace can be retrieved. The reliability of the line fitting was assessed by $R^2 = 1 - \sum_{j=1}^{n} (r_{oj} - \hat{r}_{oj})^2 / \sum_{j=1}^{n} (r_{oj} - \bar{r}_{oj})^2$, where r_{oj}, $\hat{r}_{oj}$ and $\bar{r}_{oj}$ were the measured spot sizes, fitting results and average spot sizes at each position, respectively. In this case, R^2 was 0.969 when the best fitting was obtained for $r_{i0} = 69.6\ \mu m$ and $r_m = 41.8\ \mu m$, as the dashed green line in Fig. 5(a). The accuracy in determination of r_m is related to the deviation Δr_o between the experimental data and the retrieved traces by $\Delta r_m = \sqrt{(r_{min} \pm \Delta r_o)(r_{max} \pm \Delta r_o)} - r_m$, where r_{min} and r_{max} were the extreme values of the retrieved spot size oscillation trace. By considering the maximum deviation Δr_o at all intervals at 500 ns, the lower and upper limits were calculated to be $-1.68\ \mu m$ and $1.75\ \mu m$, respectively. Therefore, the lower and upper limits of Δr_m were -1.93 and $1.98\ \mu m$, and the channel depth was $6.46^{+0.64}_{-0.57} \times 10^{16}\ cm^{-3}$.

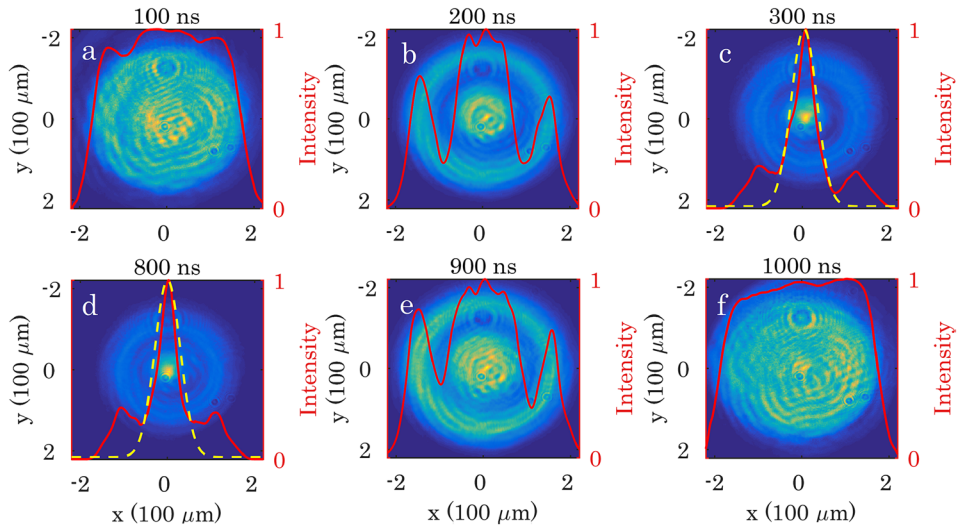

FIG. 4. Laser modes at the exit of a 2 *cm* capillary at different delays. The red traces are the normalized intensity profiles. The yellow traces are the intensity profiles by fitting the intensity of the central peak to a Gaussian form.

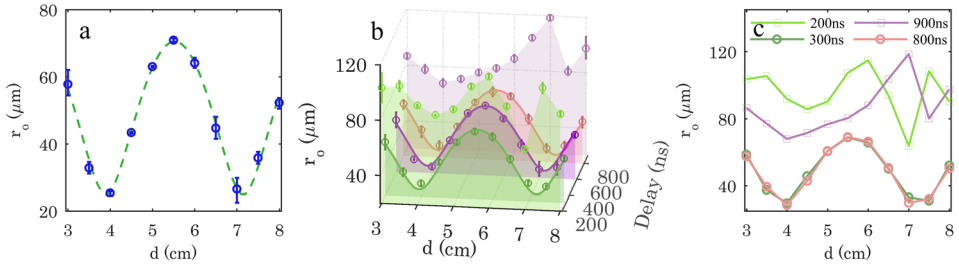

FIG. 5. (a) Spot sizes of pulse at the exit of capillaries from 3 to 8 *cm* at 500 *ns* and the retrieved oscillation trace for $r_{i0} = 69.6\,\mu m$ and $r_m = 41.8\,\mu m$ (dashed green line). (b) Measured laser spot sizes from 200 to 900 *ns* and the fitting oscillation traces from 300 to 800 *ns*. (c) Measured laser spot sizes at 200, 300, 800 and 900 *ns*.

The spot sizes (hollow circles) and the retrieved oscillation traces (solid lines) between 300 and 800 *ns* at 20 mbar are plotted in Fig. 5(b). The error bars at each point represent the deviation ranges of the experimental data from the average sizes at each interval. R^2 was above 0.96 for all the fitting. The retrieved oscillation traces from 300 to 800 *ns* were similar in shape, which also indicated that the guiding effect of the plasma on the probe light was stable. The incident laser beam waist radius (r_{i0}) from the retrieved oscillation traces between 300 and 800 *ns* is plotted in Fig. 6(a). The time averaged spot size was $70.08^{+2.16}_{-2.14}\,\mu m$. The time averaged matched spot size r_m from the oscillation traces was $42.03^{+2.43}_{-2.44}\,\mu m$, as shown in Fig. 6(b). The corresponding channel depth n_d determined from r_m was $6.40^{+0.81}_{-0.67} \times 10^{16}\,cm^{-3}$ as shown in Fig. 6(c). r_m showed a decrease trend at 300 *ns* when the discharge current was reaching its peak, which might be a result of the steep temperature gradient caused by a large current. The spot sizes measured at 200 and 900 *ns* are also plotted in Figs. 5(b) and (c). It is worth noting that the spot sizes were larger than those between 300 and 800 *ns* and had significantly different oscillation behaviors. It suggests that Eq. (2) can not describe the spot size oscillations at these two delay instances because the channel has not been formed or already collapsed. It agrees with our analysis of the laser modes in Fig. 4.

The capillary discharge waveguides under lower pressures of 5 and 15 mbar were also diagnosed using this method, whose on-axis densities were $2.4 \times 10^{17}\,cm^{-3}$ and $7.0 \times 10^{17}\,cm^{-3}$, respectively. When the on-axis density was $7.0 \times 10^{17} cm^{-3}$, the laser modes showed intense peaks between 300 and 600 ns. The retrieved oscillation traces are plotted in Fig. 7(a). R^2 was higher than 0.93 in all the cases. From the retrieved spot size oscillation trace, the time averaged incident laser beam waist radius was determined as $73.75^{+2.39}_{-2.16}\,\mu m$. The matched spot size and density depth are plotted in Figs. 7(b) and (c), with the time averaged values of $r_m = 46.0^{+2.64}_{-2.41}\,\mu m$ and $n_d = 5.34^{+0.61}_{-0.56} \times 10^{16}\,cm^{-3}$. Further, when the gas pressure decreased to 5 mbar, the channel only existed between 500 and 700 *ns*. The experimental data and retrieved traces are plotted in Fig. 7(d). The time averaged incident laser spot size was $76.49^{+2.53}_{-2.05}\,\mu m$. r_m and n_d were determined to be $48.64^{+2.78}_{-2.28}\,\mu m$ and $4.77^{+0.48}_{-0.50} \times 10^{16}\,cm^{-3}$ as shown in Figs. 7(e) and (f). Compared to the channel at 20 mbar, the plasma channel forming time at 5 and 15 mbar were 300 and 200 *ns* shorter, respectively. The matched spot sizes were ~6.6 μm and

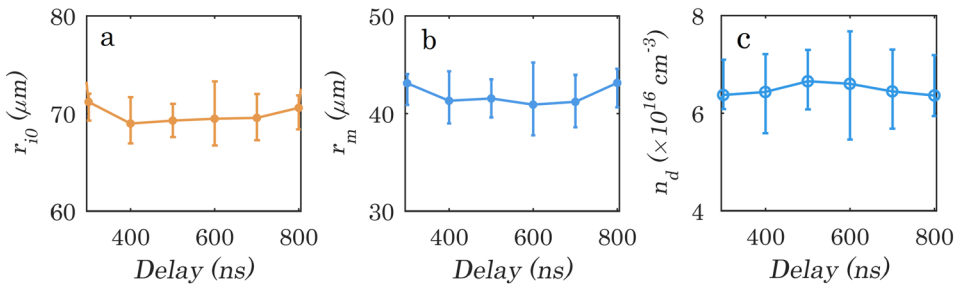

FIG. 6. (a) Beam waist radius of the incident laser, (b) matched spot size of the channel, and (c) channel depths calculated from the oscillation curve fit from 300 to 800 *ns*.

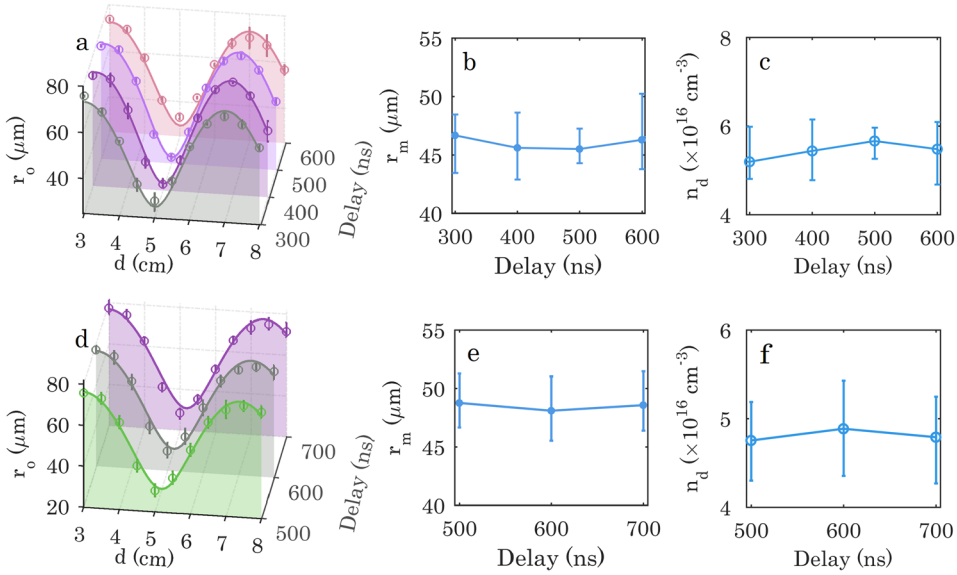

FIG. 7. Measured spot sizes and the retrieved spot size oscillation traces at (a) 15 mbar between 300 ns and 600 ns and (d) 5 mbar between 500 ns and 700 ns. (b) Matched spot sizes and (c) channel depths at 15 mbar. (e) Matched spot sizes and (f) channel depths at 5 mbar.

~4 μm wider, respectively. The matched spot size decreases in low density plasma, which might be due to the enhancement of the heating effect owing to the large resistivity in low-density plasma.[11]

Determination of r_m based on the spot size oscillation with a collimated incident laser, which is obtained by fitting the theoretical description to the spot sizes measured at the exit of capillaries of different lengths, is not sensitive to the laser divergence at the channel entrance and the solution is unique. The main error has several origins. The first one is the laser centroid offset caused by the alignment error and the pointing fluctuation, because it affects the location of the laser modes centroid at the capillary exit. The centroid determination accuracy is estimated to be ~100 μm in the experiment. The pointing fluctuation is ~1 μrad in our experiment, which can cause laser centroid offset of 100 μm.[19] These two effects will introduce errors in measuring the spot size of the laser modes. Under a 20-mbar pressure in Fig. 5, the measurement error is nearly ±2.1 μm and it lead to an error of ±2.4 μm in r_m. An improved magnification system can be used to get a smaller measurement error. Also, the accuracy of the line fitting could be improved by measuring more data at a smaller interval and setting an appropriate confidence interval. This is limited by the experimental conditions. Another error source is caused by the ~2mm density ramp at the channel exit as shown in Fig. 3(b), which might not guide the laser efficiently. The error could be estimated by assuming that the laser diffracts with a maximum exit angle in the ramp, which would cause a maximum Δr_o of ±0.86 μm in determination of the spot size. The corresponding inaccuracy in determination of r_m is nearly ±0.97 μm.

V. CONCLUSION

In conclusion, measurement of a capillary discharge waveguide based on retrieving its spot size oscillation trace is proposed in this paper. The oscillation trace is retrieved from the laser spot sizes measured at the exits of capillaries of different length with the peak electric current, capillary radius and the gas pressure fixed. The radial density has the same profile in all the capillary discharge waveguide if the three parameters are fixed. The matched spot size as well as channel depth is determined from the retrieved spot size oscillation trace. The average matched spot sizes varied from 48.64 μm to 42.03 μm when the on-axis density is increased from 2.4×10^{17} cm^{-3} to 9.7×10^{17} cm^{-3}. It provides the plasma-channel-guided LWFAs with a laser spot size reference, especially with plasma density below 1×10^{18} cm^{-3}.

ACKNOWLEDGMENTS

This work was supported by the National Natural Science Foundation of China (grant nos. 11127901, 11425418, 61521093, and 11505263), Strategic Priority Research Program (B) (grant no. XDB16), Shanghai Sailing Program (grant no. 17YF1421100), Youth Innovation Promotion Association CAS, and State Key Laboratory Program of the Chinese Ministry of Science and Technology.

[1] R. Bingham, J. T. Mendonca, and P. K. Shukla, Plasma Phys. Control. F. **46**, R1–R23 (2004).
[2] C. G. R. Geddes, C. Toth, J. van Tilborg, E. Esarey, C. B. Schroeder, D. Bruhwiler, C. Nieter, J. Cary, and W. P. Leemans, Nature **431**, 538–541 (2004).
[3] S. P. D. Mangles, C. D. Murphy, Z. Najmudin, A. G. R. Thomas, J. L. Collier, A. E. Dangor, E. J. Divall, P. S. Foster, J. G. Gallacher, C. J. Hooker, D. A. Jaroszynski, A. J. Langley, W. B. Mori, P. A. Norreys, F. S. Tsung, R. Viskup, B. R. Walton, and K. Krushelnick, Nature **431**, 535–538 (2004).
[4] K. Nakajima, Proc. Jpn. Acad. Ser. B-Phys. Biol. Sci. **91**, 223–245 (2015).
[5] C. E. Clayton, J. E. Ralph, F. Albert, R. A. Fonseca, S. H. Glenzer, C. Joshi, W. Lu, K. A. Marsh, S. F. Martins, W. B. Mori, A. Pak, F. S. Tsung, B. B. Pollock, J. S. Ross, L. O. Silva, and D. H. Froula, Phys. Rev. Lett. **105**, 105003 (2010).
[6] A. Zigler, Y. Ehrlich, C. Cohen, J. Krall, and P. Sprangle, J. Opt. Soc. Am. B **13**, 68–71 (1996).
[7] Y. Ehrlich, C. Cohen, A. Zigler, J. Krall, P. Sprangle, and E. Esarey, Phys. Rev. Lett. **77**, 4186–4189 (1996).
[8] H. Lu, M. Liu, W. Wang, C. Wang, J. Liu, A. Deng, J. Xu, C. Xia, W. Li, H. Zhang, X. Lu, C. Wang, J. Wang, X. Liang, Y. Leng, B. Shen, K. Nakajima, R. Li, and Z. Xu, Appl. Phys. Lett. **99**, 091502 (2011).
[9] A. Deng, M. Liu, J. Liu, X. Lu, C. Xia, J. Xu, C. Wang, B. Shen, R. Li, Z. Xu, and K. Nakajima, Plasma Sci. Technol. **13**, 362–366 (2011).
[10] B. H. P. Broks, K. Garloff, and J. J. A. M. van der Mullen, Phys. Rev. E **71**, 016401 (2005).
[11] N. A. Bobrova, A. A. Esaulov, J. I. Sakai, P. V. Sasorov, D. J. Spence, A. Butler, S. M. Hooker, and S. V. Bulanov, Phys. Rev. E **65**, 016407 (2002).
[12] J. Ashkenazy, R. Kipper, and M. Caner, Phys. Rev. A **43**, 5568–5574 (1991).
[13] D. J. Spence, A. Butler, and S. M. Hooker, J. Phys. B: At. Mol. Opt. Phys. **34**, 4103–4112 (2001).
[14] A. Butler, D. J. Spence, and S. M. Hooker, Phys. Rev. Lett. **89**, 185003 (2002).
[15] D. J. Spence, A. Butler, and S. M. Hooker, J. Opt. Soc. Am. B **20**, 138–151 (2003).
[16] S. M. Hooker, D. J. Spence, and R. A. Smith, J. Opt. Soc. Am. B **17**, 90–98 (2000).
[17] A. J. Gonsalves, T. P. Rowlands-Rees, B. H. P. Broks, J. J. A. M. van der Mullen, and S. M. Hooker, Phys. Rev. Lett. **98**, 025002 (2007).
[18] P. Sprangle, J. Krall, and E. Esarey, Phys. Rev. Lett. **73**, 3544–3547 (1994).
[19] A. J. Gonsalves, K. Nakamura, C. Lin, J. Osterhoff, S. Shiraishi, C. B. Schroeder, C. G. R. Geddes, C. Toth, E. Esarey, and W. P. Leemans, 14th Workshop on Advanced Accelerator Concepts **1299**, 150–155 (2010).
[20] P. S. Antsiferov, M. R. Akdim, and H. T. van Dam, Rev. Sci. Instrum. **78**, 123107 (2007).
[21] M. A. Gigosos, M. A. Gonzalez, and V. Cardenoso, Spectrochim. Acta B **58**, 1489–1504 (2003).
[22] M. Liu, A. Deng, J. Liu, R. Li, J. Xu, C. Xia, C. Wang, B. Shen, Z. Xu, and K. Nakajima, Rev. Sci. Instrum. **81**, 036107 (2010).
[23] H. Kogelnik and T. Li, Appl. Opt. **5**, 1550–1567 (1966).
[24] S. Shiraishi, C. Benedetti, A. J. Gonsalves, K. Nakamura, B. H. Shaw, T. Sokollik, J. van Tilborg, C. G. R. Geddes, C. B. Schroeder, C. Toth, E. Esarey, and W. P. Leemans, Phys. Plasmas **20**, 063103 (2013).